Role of poly(ADP-ribose) polymerase activation of immune cells in inflammatory bowel disease

Inflammatory bowel disease (IBD) is a multifactorial disease accompanied by oxidant-induced tissue injury. Oxidative damage may lead to the activation of poly(ADP-ribose) polymerase-1 (PARP-1), the highest catalytic activity member of the adenosine diphosphate ribosyl transferase (ADPRT) enzyme superfamily or PARPs. PARP-2 is the second member of the family and it is also activated by DNA-damage.

Previous studies showed elevated PARP-1 activity in the inflamed colon of the chemically and genetically induced colitis animal models The beneficial effect of PARP inhibition was also confirmed in various animal models [1,2]. A few available human studies suggested a more complex role of PARP-1 in the pathogenesis of the disease. Makowitz et al. in 1988 showed that isolated mononuclear cells of IBD patients exhibited reduced hydrogen peroxide-induced PARP-1 activation [3]. A few years later, autoantibodies against PARP-1 were identified in Crohn's disease patients [4,5]. In our previous study examining PARP-1 activation of colonic tissues in pediatric patients an elevated mRNA expression of PARP-1 was observed, however; PARP-1 protein level and activity were reduced [6].

Recent studies also suggested the involvement of dysregulated T-cell response in the pathogenesis of Crohn's disease. Especially helper T cells (CD4+ T or Th cells) seems to play a pathogenic role in CD. Abnormal Th1 activation, increased Th17 and reduced regulatory T cell (Treg) activity is characteristic in CD [7,8]. PARP-1 and PARP-2 also plays important role in the regulation of T-cell response. PARP inhibitors and genetic downregulation of PARP-1 or PARP-2 may lead to decreased Th17 and increased Treg numbers and activation. These effects were shown to be beneficial in animal models of certain autoimmune diseases (rheumatoid arthritis, encephalomyelitis) [9,10].

Although the role of PARPs is not completely elucidated in the pathogenesis of IBD, the use of PARP inhibitors in the clinical treatment of IBD have been proposed by several scholars[11], mainly based on the preclinical animal studies showing beneficial effects. PARP inhibitors are already in the clinical practice in the maintenance therapy of various solid tumors mainly with BRCA mutation. On the other hand, the T cell function modulating effect of PARP inhibitors is one of the possible cause of the present or emerging resistance to PARP inhibitor therapy[12].

Our major aim was to investigate the role of PARP-1 and PARP-2 in the pathogenesis of inflammatory bowel disease. Our goal was to examine how systemic and hematopoietic PARP-1 and PARP-2 activity affects inflammatory processes and the development of experimental colitis.

I. First, we examined how does PARP-2 downregulation in T cells influence the lipopolysaccharide (LPS)-induced inflammation of the large intestine. Our results have been published in 2023 in Frontiers Immunology.
II. We also examined the effect of the combined global PARP-1 and T-cell specific PARP-2 downregulation on the condition of the large intestine. The manuscript is ready for submission.
III. The novel combination therapy of PARP inhibitors and immune checkpoint inhibitors for the maintenance therapy of ovarian cancer is based on the observed effect of PARP inhibitors on T cell response. We performed a systematic review and meta-analysis based on the available human studies. The manuscript is ready for submission.
IV. Although the clinical use of PARP inhibitors in IBD was proposed, no previous systematic review and meta-analysis is available about the preclinical animal models. We initiated a systematic review and meta-analysis, which is in the phase of data collection. We plan to complete the review in July 2024.
V. The grant was also cited in seven other published articles in related fields.

I. Bencsics M, Bányai B, Ke H, Csépányi-Kömi R, Sasvári P, Dantzer F, Hanini N, Benkő R, Horváth EM. **PARP2 downregulation in T cells ameliorates lipopolysaccharide-induced inflammation of the large intestine.** Front Immunol. 2023 Jun 30;14:1135410. doi: 10.3389/fimmu.2023.1135410. **(IF: 7.3)**

In summary, T cell specific PARP2 knock-out (T-PARP2-KO) managed to dampen the inflammation induced by LPS injection, which was reflected by much milder inflammatory responses evaluated by the histology scores, lower local oxidative stress reflected by immunohistochemistry against 3-nitrotyrosine and unchanged or even suppressed local inflammatory cytokines levels such as TNFα, IL-1β and IL-17, compared to the counterpart where a much more intense inflammatory response could be observed on the previously mentioned 3 aspects. Accompanied with the remitted inflammation in T-PARP2-KO animals altered inflammatory signaling transductions were observed, reflected by decreased p42/44 Erk activation and NF-κB level, as well we markedly suppressed PARP1 activity which was reflected by significantly lower general protein and auto-PARrylation. Concerning the cellular response, LPS treatment managed to raise the helper T cell ratio independent of genotype but only in T-PARP-2 KO animals a significant decrement of regulatory T cells (Treg) count in the periphery was observed, accompanied by the significant increment of Treg density in the intestinal mucosa which was absent in control animals after LPS treatment. Such differences in T cell response may have provided the hint that increased local recruitment and conversion of Treg were playing a role in the amelioration of acute inflammation in T-PARP2-KO animals.

II. Chronic intestinal inflammation in a murine model with global PARP-1 and T-cell specific PARP-2 deficiency (manuscript is ready to be submitted, some data were presented in diploma thesis)

Downregulation of PARP-1 with either pharmacological inhibition or genetic modification has been proven to be beneficial in various inflammatory conditions, including experiment-induced colitis (with either di-/ trinitrobenzene sulfonic acid or dextran sulfate) in the purpose of studying IBD. In our previously published study, T cell specific PARP-2 deficiency was also proven to be beneficial in dampening acute inflammatory responses induced by intraperitoneal lipopolysaccharide injection. The rodent model combining both genetic modification, a global PARP-1 deficiency background plus T cell specific PARP-2 knock-out (so-called double knock-out animals, DKO animals) were developed previously by Navarro et al., in the aim of revealing faulty immune responses of T cells against viral infection and cancer cells. Taking account of the suppression of intestinal inflammatory responses from either PARP deficiency and meanwhile the abundance of lymphatic tissue in the intestine, it is worthwhile to further research the effect of combining deficiency of both PARP homologs on the intestines
T-cell-PARP-2 knock-out with global PARP-1 depletion (CD4-Cre, PARP1-/-, PARP2f/f), so-called double-knock-out (DKO) mice were generated from crossbreeding of single-knock-out mice with either PARP-1 deficit (CD4-Cre, PARP1-/-, PARP2+/+) or T-cell specific PARP-2 knock-out (CD4-Cre, PARP1+/+, PARP2f/f). Control animals bear CD4-Cre recombination but no loxP site on PARP-2 exons (CD4-Cre, PARP1+/+, PARP2+/+). Male mice aged 14 to 18 weeks were anaesthetized (N=22), Large intestines of male mice aged 14 to 18 weeks were collected after physiological saline perfusion under deep anesthesia placed in phosphate buffered formaldehyde or snap frozen in fluid nitrogen and stored at -80°C. Histological evaluation was performed on hematoxylin and eosin (Sigma-Aldrich, St. Louis, MO, USA) stained tissue sections (5μm, paraffinized). The histology of intestines was evaluated based on a scoring system modified from the system published by Bita Naini and Galen Cortina[13]. The three aspects of colonic inflammation comprised of crypt architecture distortion, lymphoplasmacytosis, presence of cryptitis and crypt abscess were evaluated on each specimen

with point given from 0-2 according to the extent of each parameter and then summed up afterwards, which resulted in a score ranging from 0-6 (The 4 segments of large intestines – cecum, ascending, transverse and descending colons were all evaluated based on this system and the scores from each segments were summed up) (Table 1.). Hematoxylin-eosin stained CD3 and CD20 labeled sections were evaluated by an independent pathologist to exclude other reasons for immune cell accumulation.

Table 1. Histology scoring of chronic inflammation

Histologic features	Definitions	Scoring
crypt architectural distortion	Irregularly arranged, branched crypts, irregular crypt outlines, atrophy and crypt shortening, surface villiform changes	0 - absent 1- mild 2- conspicuous
lymphoplasma-cytosis	Range: subjective increase in lymphocytes and plasma cells particularly at the base ≥ upper and middle thirds (mild) to band-like collections separating crypts from muscularis mucosae (conspicuous)	
cryptitis and crypt abscess	Range: rare examples of neutrophilic infiltration of the epithelium (mild) up to frequent marked crypt involvement by neutrophils (conspicuous)	

The extent of lipid peroxidation reflects the local level of highly active oxidants. In our study we investigated the level of 4-hydroxynonenal (HNE) in the mucosa from separate segments of colon: cecum, ascending, transverse and descending colons with immunohistochemistry. Deparaffinized samples were stained with anti-HNE antibody (ab46545, Abcam, Cambridge, UK; RRID: AB_722490, 1:200), anti-CD3 and anti-CD20 antibodies (1:100, Dako FLEX, Glostrup, Denmark), FoxP3 (14-5773-82) rat monoclonal IgG2a kappa antibody 1:500, (Invitrogen, Massachusetts, USA). Horseradish-peroxidase-linked anti-rabbit polyclonal horse antibodies (MP-7401-15, Vector Laboratories, California, USA) were used for the secondary labelling during immunohistochemistry and the visualization was achieved by grey-black-colored diamino-benzidine with nickel (Ni-DAB, SK-4100, Vector Laboratories), or brown-colored DAB with hematoxylin counterstaining. Images of the immune-labeled specimens were obtained with Nikon Eclipse Ni Microscope (Nikon Instruments, Amstelveen, The Netherlands) with a 20× objective lens, using a Nikon DS-RI2 camera and NIS-Elements BR imaging software (Nikon Instruments). Quantifying evaluation was achieved by measuring non-calibrated optical density of the grey-black color in case of HNE (Ni-DAB) in the mucosa with ImageJ Software (National Institutes of Health, Bethesda, MA, USA). Evaluation of CD3 immunohistochemistry was finished with visually counting the positively stained cells in randomly selected high power fields (HPF, with 40x magnifying object lens). 5 HPFs were randomly chosen on each segment of intestines and counted by 2 blinded independent researchers, to whom the specimens were randomly assigned. Normalization was guaranteed in the way that during capturing images only intestinal mucosa was included and when capturing blank space was inevitable, ImageJ Software (National Institutes of Health, Bethesda, MA, USA) was implemented to crop out the blank area, meanwhile the ratio of surface area and HPF was calculated, to which CD3 positive cell density was normalized. The mean values of 5 HPFs were utilized to evaluate the CD3 positive cell density in the intestinal mucosa. Foxp3 positively stained cells were counted in the whole cross-section of the intestinal segment, and the number was normalized to the epithelial area using ImageJ Software.

Inflammatory cytokine concentrations from distal colon homogenates were measured using the ELISA method (TNFα- Invitrogen Mouse TNFα ELISA Kit BMS607-3 and IL1β -Invitrogen Mouse IL-1 beta ELISA Kit BMS6002) (Thermo Fisher Scientific), and normalized to total protein content, each group contained 4-6 animals.

Tissue HNE-modified protein, PARP-1, PARP-2 protein level and PARP activity (level of protein PARylation) were investigated by Western blotting in 4 to 8 animals per group. Supernatants of the lysates were boiled at 95°C for 5 minutes in reducing SDS sample buffer and the samples with equal protein mass were run on 4–12% (w/v) gradient polyacrylamide gels for separation, and subsequently transferred to nitrocellulose membrane (Invitrogen). Membranes were incubated overnight (at 4°C) respectively with anti-HNE antibody 1:1000 (ab46545, Abcam, Cambridge), the anti-PAR binding reagent 1:1000 (MABE1031, Sigma-Aldrich, St. Louis, MO, USA; RRID: AB_2665467), anti-PARP-1 antibody 1:1000 (ab191217, Abcam, Cambridge, UK; RRID: AB_2861274), anti-PARP-2 antibody 1:500 (GTX01558, GeneTex, Irvine, USA), anti-Bak antibody (1:500, 06-536, Merck Millipore Darmstadt, Germany) . HRP-conjugated secondary antibody (1:1000 in 1% milk) (goat anti-rabbit HRP Invitrogen catalogue #31460) and Pierce™ ECL Western Blotting Substrate (Invitrogen #32109) was used for visualization. Beta-actin was used as a loading control (ab49900 1:10000 in 1% milk; Abcam, RRID: AB_867494). Band and column intensity was evaluated by Image Lab Software (Bio-Rad, Hercules, CA, USA)

Members of the intracellular inflammatory signal transduction were examined by Western blotting in 3-4 animals per group. Supernatants of the homogenates were boiled at 100°C for 5 minutes in reducing SDS sample buffer and each sample with equal protein mass was run on 4-15% (w/v) gradient polyacrylamide gels (Bio-Rad). Separated proteins were transferred to the nitrocellulose membrane (Bio-Rad). To prevent non-specific labelling, the membranes were blocked for 10 minutes in EveryBlot blocking buffer (Bio-Rad), then incubated with the following monoclonal antibodies: p38 MAPK (#9212S; Massachusetts RRID: AB_330713), phospho-p38 MAPK (#4511S; RRID: AB_2139682), p44/42 ERK (#4695S; RRID:AB_390779), phospho-p44/42 ERK (#4370S;RRID: AB_2315112),NF-kB p65 (#8242S; RRID: AB_10859369), (Cell Signaling, Danvers, MA, USA) in 1:1000 dilution overnight at 4°C. Bound antibody was detected with enhanced chemiluminescence after incubating in horseradish peroxidase-conjugated anti–rabbit-IgG (from donkey) secondary antibody (GE Healthcare, Chicago, Illinois, USA,NA934V) in 1:5000 dilution (1 hour, room temperature). Beta-actin was detected with the use of HRP-linked anti-actin antibody (ab49900, Abcam; RRID: AB_867494). Band intensity was quantified by the ImageJ software (ver. 1.53o). The films were scanned at 600 dots per inch in TIFF format. Each band was individually selected and the peak area was acquired and quantified as arbitrary area values of each histogram thrice.

Data analysis was performed by GraphPad statistical software package (GraphPad Software, La Jolla, CA). Statistical probes were based on two-way ANOVA/mixed model analysis with Tukey's post hoc test, and optical density values were log-transformed for analysis. $p<0.05$ was considered statistically significant. Data are presented as mean ± standard deviation (SD). N represents the number of animals per group.

In comparison to animals from the other three groups, DKO animals exhibited features resembling chronic inflammation, among which lymphoplasmacytosis has been shown to be the most prominent, while crypt architectural distortion and cryptitis or crypt abscess were less frequently seen in histological examinations (scoring system in Table 1.). DKO animals had significantly higher inflammatory scores compared to other groups with $p<0.0001$ in all comparisons (Figure 1.).

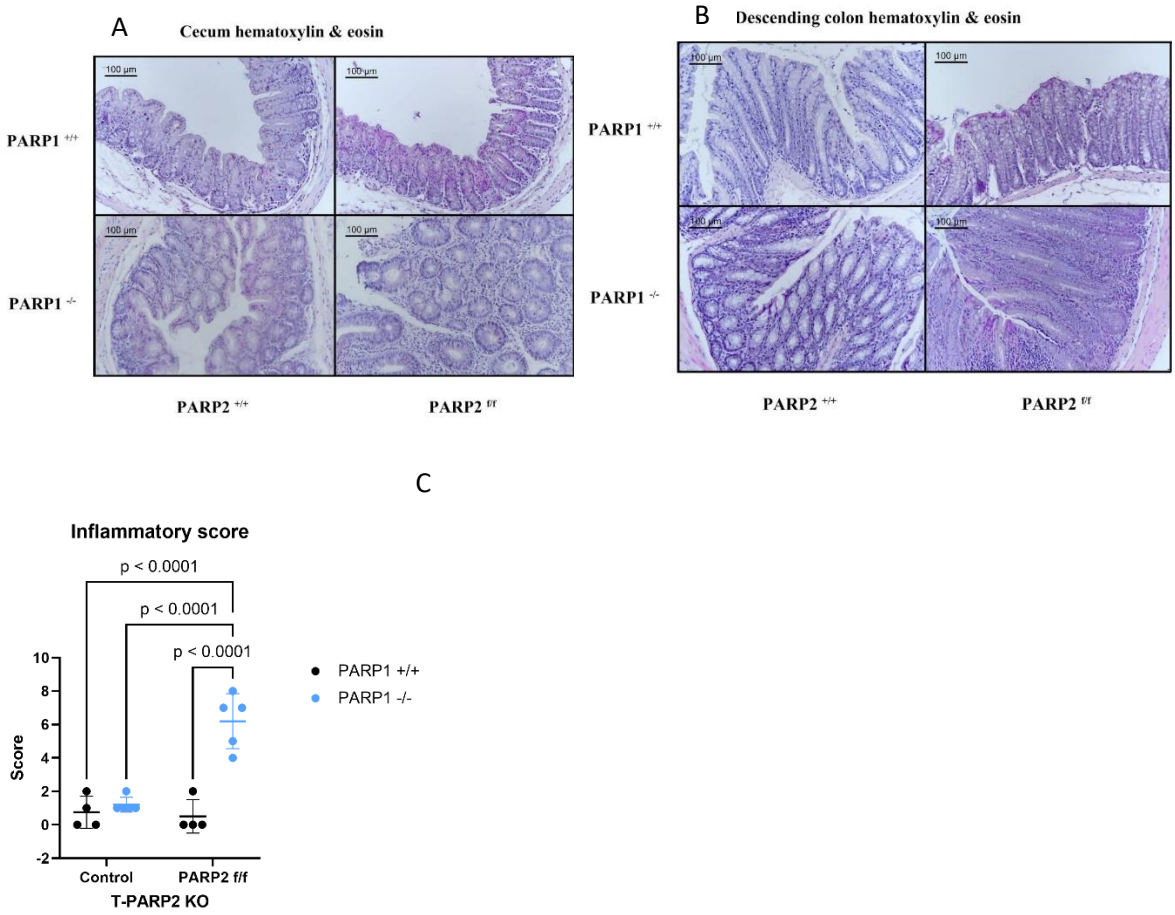

Figure 1. Inflammation in the large intestines. Panel A. Representative histological images of cecum of each genotype with hematoxylin & eosin staining. Scale bar is 100µm. Prominent lymphoplasmacytosis can be observed in PARP1-/- PARP2 f/f genotype. Panel B. Representative histological images of descending colon of each genotype with hematoxylin & eosin staining. Scale bar is 100µm. Prominent lymphoplasmacytosis can be observed in the PARP1-/- PARP2 f/f genotype. Panel C. inflammatory score of each genotype group, DKO animals (PARP-1-/-, PARP-2f/f) have significantly higher scores compared to the other 3 groups. Data were analysed with two-way ANOVA (PARP1, PARP2) with Tukey's post-hoc test and p is shown on the graph for each group. N=4-5 per group.

CD3 positive cells were significantly higher in DKO animals compared to other 3 genotypes; however, PARP1 -/- groups (including PARP1 knock-out and DKO group) showed elevated Treg count in the intestine, which is expected on account of PARP1 KO promoting the conversion of Th0 to Treg (by enhancing Foxp3 expression) (Figure 2.)

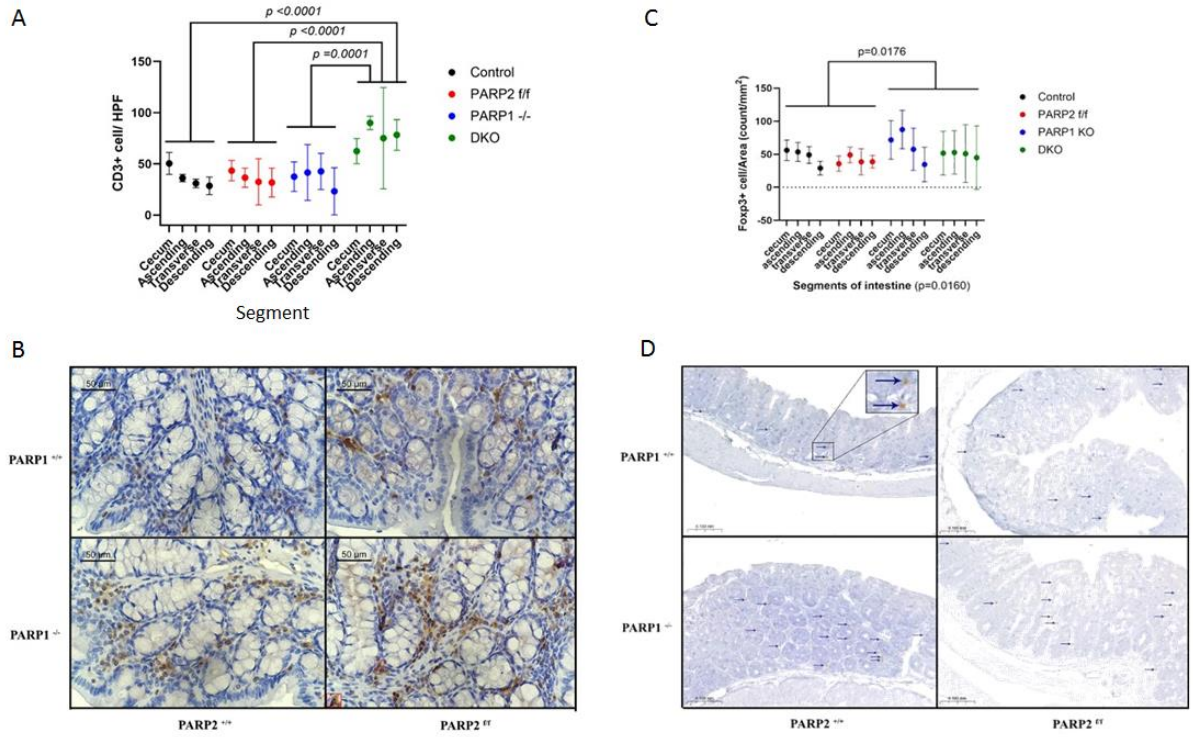

Figure 2. Evaluation of CD3 and Foxp3 positive cells in the intestinal mucosa.

Panel A: Results of CD3 positive cell count per HPF. CD3 positive cell count was significantly higher in DKO animals compared to the other 3 groups. Data were analyzed with two-way ANOVA (PARP1, PARP2) with Tukey's post hoc test and p is shown on the graph for each group N=2-4 per segment per group. Panel B: Representative images of CD3 positive immunohistochemistry staining in the ascending colons of animals from each group. The images were captured with 40x magnifying power. Brown color represented positive stained cells. Red rectangle encircled one example of positive stained cell in DKO specimen, which were magnified in the left lower corner. Panel C: Results of Foxp3 positive cell count normalized to surface area of intestinal mucosa. PARP1 knock-out bearing groups (PARP1 knock-out and DKO) showed higher level of Foxp3(+) cell density and significant difference between segments of intestines was detected. Data were analyzed with three-way ANOVA (PARP1, PARP2, Segment of intestines) with Tukey's post hoc test and p is shown on the graph for each group. N=4-6 per group. Panel D: Representative images of Foxp3 positive immunohistochemistry staining. The images were captured with 20x magnifying power. Brown color represented positive stained cells which were indicated by blue horizontal arrows (shown as in left upper image with magnified view of positive cells.)

4-Hydroxynonenal immunohistochemistry revealed significantly higher levels of 4-HNE in the cecum of DKO animals, compared to the same segments from control and T-PARP-2-KO animals. Similar trends of 4-HNE levels are seen in other segments of intestines, while not reaching statistical significance. However, protein lysates showed no between-group differences of HNE-modified protein level (Fig. 3.)

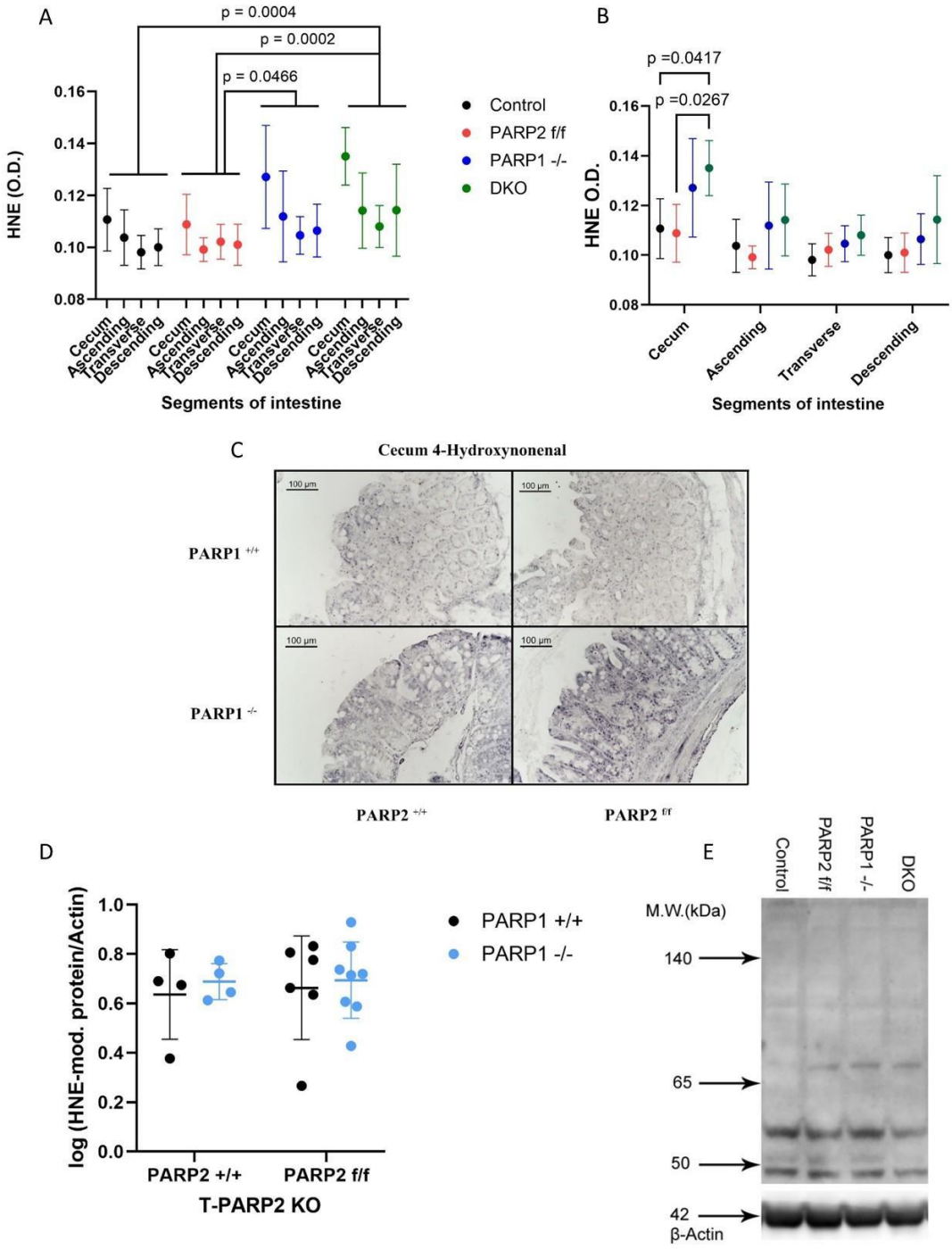

Figure 3. Evaluation of lipid peroxidation by measuring HNE production with immunohistochemistry and HNE-modified protein by Western-blot. Panel A: HNE immunohistochemistry result evaluated according to genotype. PARP1 knock-out group had significant higher level of HNE compared to T-PARP2 knock-out group while DKO animals had significant higher level of HNE in comparison to both control and T-PARP2 knock-out groups. The results were analyzed with two-way ANOVA with Tukey's post hoc test, p values were noted on the graph for each group. Panel B: HNE immunohistochemistry result evaluated regarding segments. In the cecum DKO animals exhibited significant higher HNE production compared to both control and T-PARP2 knock-out animal groups. The results were analyzed with mixed-effect analysis (two-way ANOVA, Genotype & segments of intestines) showing the

result in each segment of intestines. N=4-6 per group Panel C: Representative images of HNE immunohistochemistry. The blue-black color represents the positive staining against HNE in the cecal epithelium. Panel D: Evaluation of HNE-modified protein content from intestinal lysate supernatant. No obvious difference could be detected among 4 genotypes. The results were normalized to actin level for the same sample. Panel E: Representative image of Western-blot detecting HNE-modified protein. The evaluation range was from the first identifiable band with highest molecular weight(>140kDa) until band at around 50kDa. Data were analyzed with two-way ANOVA (Panel B: repeated measuring ANOVA) with Tukey's post hoc test and p is shown on the graph for each group. N=4-6 per group.

The images and statistical results of Western-blot evaluating levels of PARP homologues and tissue PARylation are shown on Figure 4. PARP-1 levels were significantly low in PARP1-/- mice as expected, including PARP-1 KO and DKO, compared to control and T-PARP-2-KO mice and PARP-1. PARP-2 levels in the intestines did not show significant variation between groups. Concerning PARylation level, despite the absence of PARP-1, which is responsible for the majority of catalytic activity intracellularly, in PARP-1 KO and DKO animals, the PARylation levels in the intestines did not differ obviously when comparing any two groups.

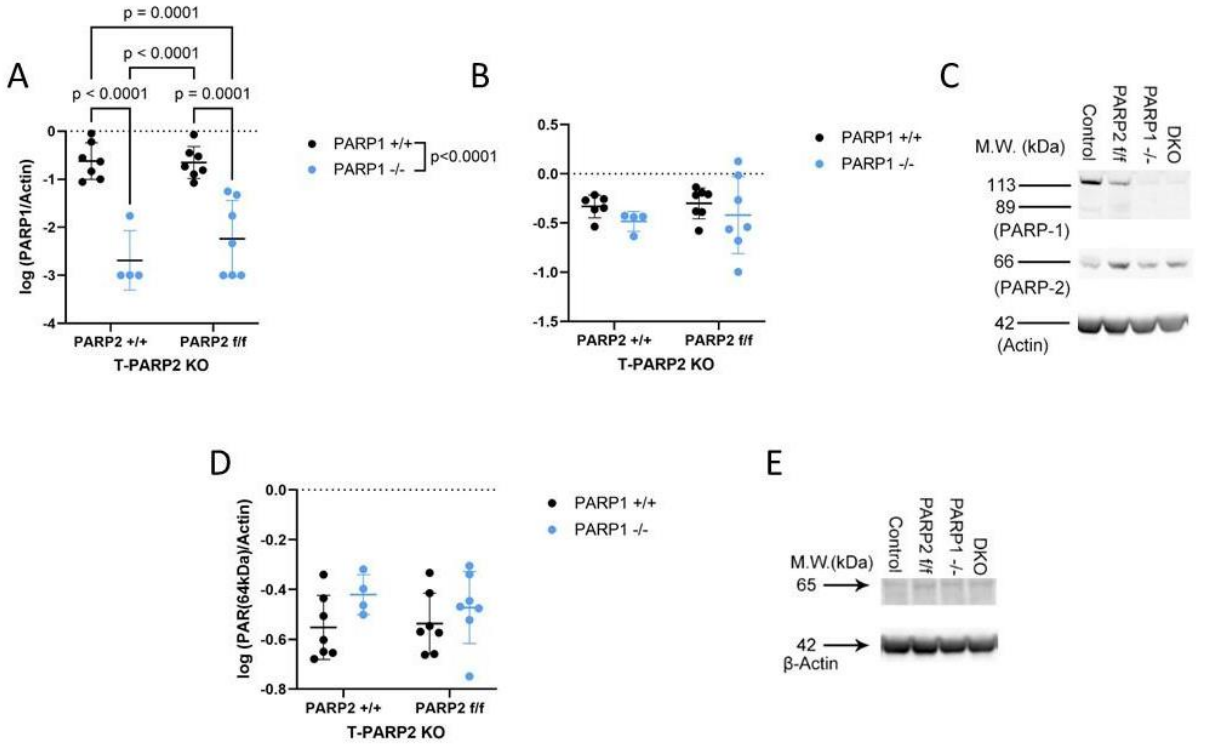

Figure 4. Evaluation of Poly(ADP-ribose) and PARP homologs content with Western-blot. Panel A: Results of PARP1 content evaluation. Groups with PARP1 knock-out genetic modification, including PARP1 knock-out and DKO, showed significantly lower PARP1 level as expected.

Panel B: Results of PARP2 content evaluation. No significant difference could be observed among groups. Panel C: Representative image of PARP1 and PARP2 Western blot. PARP1 was detected at 113 and 89 kDa (uncleaved and cleaved PARP1) and PARP2 was detected at 66kDa. The results were normalized to the actin level for the same sample. Panel D: Results of poly(ADP-ribose) level evaluation. No obvious difference was found among 4 groups. Panel E:

Representative image of Poly(ADP-ribose) western-blot. General protein PARylation was detected at 64kDa level. The results of western-blot were normalized to actin level for the same sample. Data were analyzed with two-way ANOVA (PARP1, PARP2) with Tukey's post hoc test and p is shown on the graph for each group. N=4-8 per group.

PARP2 f/f showed significant lower level of Bak compared to DKO, showing a significant interaction, which can be considered compatible with the anti-inflammatory effect of PARP2 f/f/ and auto inflammation in DKO (Fig. 5.)

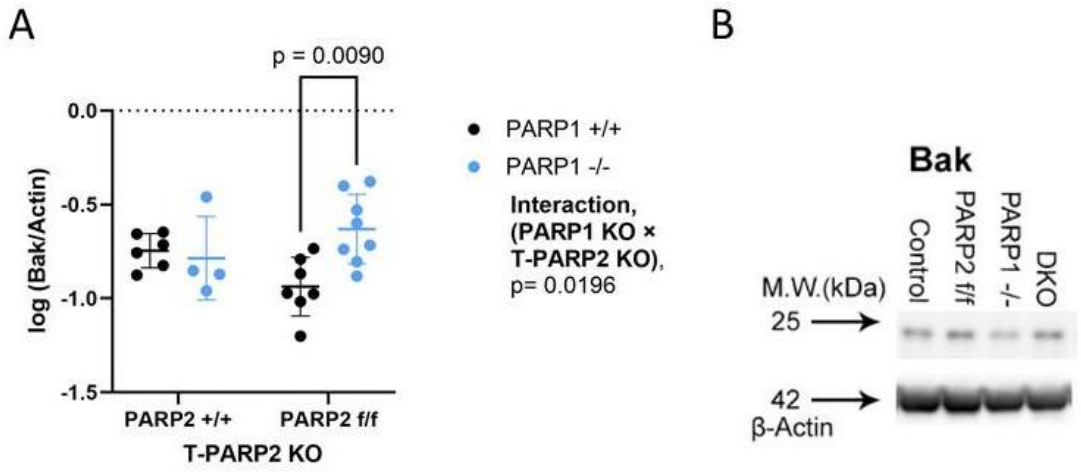

Figure 5. Evaluation of Bcl-2 pro-apoptotic protein Bak level by Western-blot. Panel A: Results of Bak level evaluation. T-PARP2 knock-out animal showed significant lower level of Bak compared to DKO animals while no other difference was detected, showing a significant interaction between PARP-1 knock-out and T-PARP2 knock-out. The results of western-blot were normalized to actin level for the same sample. Panel B: Representative image of Bak Western-blot. Bak was detected at 25kDa. Data were analyzed with two-way ANOVA (PARP1, PARP2) *with Tukey's post hoc test and p is shown on the graph for each group. N=4-8 per group.*

Tissue pro-inflammatory cytokine TNFα level showed no difference between groups of all 4 genotypes. Significant interaction from global PARP-1 and T-cell specific PARP-2 deficiency was observed: PARP-1 sole deficit resulted in the tendency of decreased baseline TNFα level while when PARP-1 deficit was combined with T-cell PARP-2 deficit the baseline TNFα level showed the tendency of increment. The results of TNFα level were shown in Figure 6. For IL-1β the cytokine level was not determined due to low cytokine levels (Data not shown).

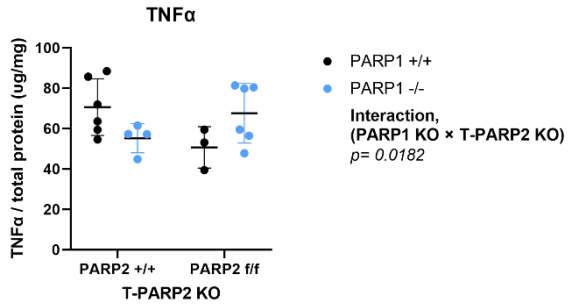

Figure 6. Tissue TNFα level from intestinal homogenates supernatant. No significant difference was observed. Data were analyzed with two-way ANOVA (PARP1, PARP2) *with Tukey's post-hoc test and p is shown on the graph for each group. N=4-5 per group.*

Levels of intracellular inflammatory signaling members showed distinct patterns when PARP-1 deficit was solely present or in combination with T-cell PARP-2 deficit. For p38 Mitogen-activated protein kinase (MAPK) , the total amount of MAPK showed no significant difference between groups, while the activation of MAPK, which is reflected by phosphorylation level of MAPK (pMAPK / tMAPK), was upregulated in PARP1-/- single deficit mice compared to control animals (p=0.029) but in DKO animals PARP-1 deficit did not result in elevated MAPK activation compared to T-PARP-2-KO animals instead, indicating an significant interaction between PARP1-/- and PARP2f/f genotypes. For p42/44 Erk, PARP-1 deficit resulted in significant increment of the total amount of Erk (normalized to actin) in mice compared to the counterparts with identical PARP-2 genotype ($PARP1^{-/-}$ vs. Control & DKO vs. $PARP2^{f/f}$). Besides, DKO animals also have a significantly higher total Erk level in comparison to control animals. The activation of Erk, evaluated by Erk phosphorylation was not significantly different in the experimental groups. The level of NF-κB showed no obvious difference between groups (Figure 7.)

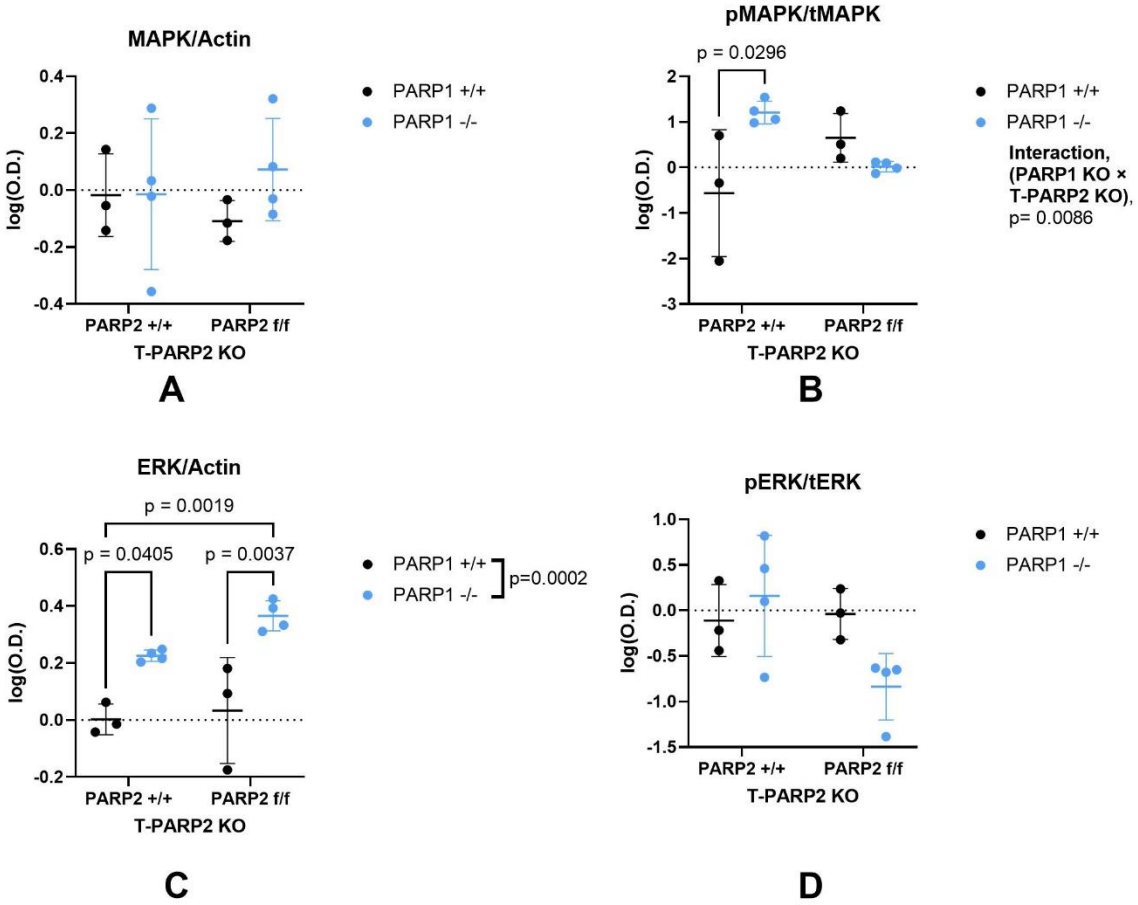

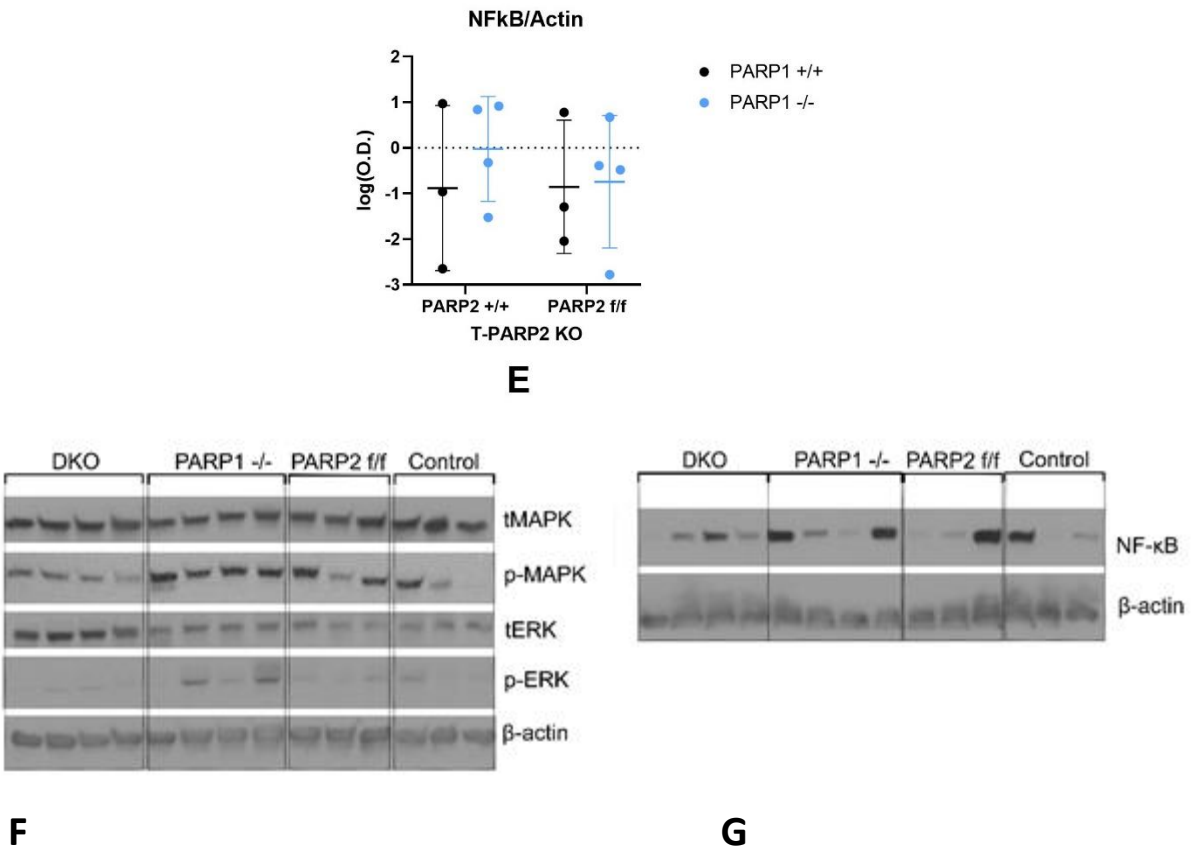

Figure 7. Examination of level of intracellular inflammatory signaling transduction members. Graph A: total p38 MAPK level normalized to smooth muscle actin showed no difference between groups Graph B: MAPK activation reflected by pMAPK/tMAPK, PARP-1 single deficient mice had significantly higher MAPK activation and interaction between PARP-1 KO and T-PARP-2 KO was also significant. Graph C: total p42/44 Erk level normalized to actin. Erk levels were significantly higher in PARP-1 deficient animals compared to counterpart animals bearing the same PARP-2 genotype. Graph D: Erk activation reflected by Erk phosphorylation. No significant effect of genotypes was observed. Graph E: level of NF-κB showed no obvious difference between groups. Panel F: Representative images from results of Western blot evaluating intracellular inflammatory signaling transduction members. Membrane F. Total MAPK (tMAPK: 38 kDa), phospho-MAPK (p-MAPK: 38 kDa), total ERK (t-ERK: 42-44 kDa), phospho-ERK (p-ERK: 42-44 kDa), β-actin (42 kDa). Panel G: Membrane G. Nuclear factor kappa B (NF-κB: 65 kDa), β-actin (42 kDa). Data were normalized and evaluated with two-way ANOVA with Tukey's post-hoc test and p is shown on the graph respective to significance. N= 3-4 per group.

In our study, DKO animals exhibited possible chronic inflammatory responses in the large intestines with unconventional features. Despite the striking histological alterations as lymphocytes infiltration and structural abnormality, as well as increased tissue oxidative stress, local cytokine level did not show significant corresponding changes and the intracellular inflammatory signaling cascade also exhibited altered reactions other than conventional inflammation. Besides, PARP activity was also found to be surprisingly similar between DKO animals and other 3 counterparts and the apoptotic profile of the DKO animals was also insignificant from control or PARP-1 knock-out groups.

III. The novel combination therapy of PARP inhibitors (PARPi) and immune checkpoint inhibitors for ovarian cancer: a single arm meta-analysis and systematic review (PROSPERO 2024 CRD42024504589) (manuscript is ready to be submitted, some data were presented in diploma thesis)

The regulatory role of PARP1 and PARP2 in T lymphocyte function may not only be important in inflammatory bowel diseases and certain other autoimmune disease, but also in cancer therapy. The use of PARP inhibitors in the maintenance therapy of various solid tumors is getting widespread in the clinical practice especially in BRCA mutant cancers. On the other hand, therapy resistance can be present or may develop during treatment, in which T cells may play a pivotal role [12]. This hypothesis is supported by preliminary studies indicating that immune check point inhibitors (ICIs) could delay or prevent the development of resistance to PARP inhibitors and PARP inhibitors could enhance the effectiveness of ICIs, even in non-BRCA mutant tumors. Immune checkpoints are regulatory, mainly inhibitory pathways involved in the regulation of inflammatory responses and are crucial in the maintenance of self-tolerance. One of these immune checkpoints is the interaction of the programmed cell death protein 1 (PD-1) and its ligands PD-L1 and PD-L2. PD-1 is expressed on T cells and initiates inhibition when binding to PD-L1 or PD-L2 on tumor cells or antigen-presenting cells. ICIs mainly act by inhibiting the interaction of checkpoint proteins and their ligands. PARP inhibitors may upregulate PD-L1 expression leading to suppressed T-cell function and reduced anti-tumor immune response, inhibiting this with ICIs may increase the efficacy of PARP inhibitors and prevent PARPi resistance. Viewed from the other side, PARPi increase the rate of DNA mutations in tumor cells leading to the increased expression of immune reactive antigens on their cell surface, leading to increased anti-tumor immune response. This change in immune environment of the tumor may increase the efficacy of ICIs [14].

Ovarian cancer is an outstanding example of solid tumors where PARP inhibitors may provide substantial benefit in maintenance therapy. The PARPi Olaparib was approved by the FDA in 2014 in advanced ovarian cancer with germline BRCA mutation after at least three prior chemotherapy regimens. Than in 2019 it was approved for first-line maintenance therapy. Recently the idea of possible combination therapies was tested in pre-clinical and clinical trials to increase the effectivity of PARP inhibitors and overcome PARPi resistance including ICIs.

As of recently, there are no existing meta-analyses analyzing the efficacy and safety of the PARPi and ICI combination therapy on ovarian cancer. Our aim was to summarize and evaluate the current evidence on the effectiveness and safety of combining PARP inhibitors with ICIs in treating ovarian cancer. Additionally, we examined the impact of genetic variations, expression patterns and platinum resistance on the efficacy of combination therapy. (PROSPERO registration: PROSPERO 2024 CRD42024504589)

PICO (Population, Intervention, Comparison, Outcome) framework was applied to determine study eligibility. Due to the low number of available controlled trials, including control arms like PARPi or ICI monotherapy, we performed a single arm meta-analysis. The population was patients with ovarian cancer. The intervention was the combination therapy of PARPi and ICI. Due to single arm analysis, there was no comparator. Outcomes were objective response rate (ORR), disease control rate (DCR), clinical benefit rate (CBR), progression-free survival (PFS), overall survival (OS), and rate of adverse events (AE) if available.

Studies that evaluated the response of ovarian cancer to the treatment based on the RECIST (Response Evaluation Criteria in Solid Tumors) 1.1 guidelines were included. Randomized controlled trials, non-randomized trials and single arm studies were included. From the non-randomized and randomized controlled trials, relevant arms were included. From studies examining multiple cancer types, data of ovarian cancer patients were included. Studies that allowed the previous treatment of PARPi or ICI were also included. Excluded studies were case reports, cross-sectional studies, meta-analyses, systematic reviews, and animal studies.

All patients with ovarian cancer were included. Patients with fallopian tube or peritoneal cancer were not included, although the histology of the three cancers is similar. There were no limitations as to newly diagnosed, advanced, or recurrent disease. Patients were included regardless of platinum sensitivity or genetic mutation. Minimum performance status (e.g., ECOG score of 0-2) and at least 12 weeks (about 3 months) of life expectancy was required. Adequate organ function and laboratory values were also required to ensure patient safety and treatment tolerance. Adolescents, mainly under 18 years of age (depending on the country where the study was performed: 18 or 19 or 21 years of age), were excluded. Patients with previous history of severe hypersensitivity reactions to similar treatments, severe prior immune-related adverse events were also excluded. Central nervous system metastases within a certain timeframe and history of invasive malignancies were also reasons for exclusion. Grounds of exclusion included conditions such as inflammatory bowel disease, myelodysplastic syndrome, acute myelogenous leukemia, primary immunodeficiency, infectious diseases like HIV or hepatitis B or C, and use of immunosuppressive medication within a specified period. Patients with previous cerebrovascular events, high cardiovascular risk, abnormal blood cell counts, and liver function were also excluded. Pregnant or breastfeeding women were excluded due to potential risks to the fetus or infant.

Selection strategy Systematic search was done in MEDLINE (via PubMed), Embase, and Cochrane Central Register of Controlled Trials (CENTRAL) from inception until the 22nd of January 2024. We used a predefined search key with keywords for PARPi and ICI. No filters were applied during the initial search. There were no language restrictions. The search key was the following: ("poly (ADP-Ribose) polymerase" OR "parp" OR “Veliparib” OR “Olaparib” OR “Talazoparib” OR “Niraparib” OR “Rucaparib” OR “Fluzoparib”) AND ("immune checkpoint" OR "PD-L1" OR “PD-1” OR "CTLA-4" OR "Immunotherapy" OR “Atezolizumab” OR “Pembrolizumab” OR “Nivolumab” OR “Durvalumab” OR “Ipilimumab” OR “Cemiplimab” OR “Avelumab” OR “Tislelizumab” OR “Dostarlimab” OR “Camrelizumab” OR “Cetrelimab” OR “Tremelimumab”). We did not include the keyword “ovarian cancer” in the search key, as some studies included multiple types of cancers, and thus those studies would be filtered out with the keyword “ovarian cancer”. The search findings were organized through EndNote 21, which included an automated and manual process to eliminate repeated records. Initial filtering was done based on the titles and abstracts by Sun June Park (SJP) and Eszter Mária Horváth (EMH). This was followed by a thorough review of the full texts. Any inconsistencies in selection were addressed and resolved by Máté Bencsics (MB) (Figure 8.) Cohen’s k for title and abstract selection was 0.81, while for whole text it was 1.

The following data were extracted from articles: title, first author, year of publication, study design, number of centers, main study findings, interventions, and outcomes. Dichotomous outcomes like objective response rate (ORR), disease control rate (DCR), presence of adverse events, and progression-free survival (PFS) were summarized. Other outcomes like clinical benefit rate (CBR), and overall survival (OS) were not included in more than two studies or were not available. Not all studies provided readily available data on the outcomes; some had to be extracted manually by analyzing the figures given in the article and the supplementary data. The collected data was stratified according to the categorical variables given to carry out subgroup analysis. Those subgroups included 1) BRCA mutated (BRCAm), BRCA wild-type/HRD positive (BRCAw/HRD+), HRD negative (HRD-), 2) PD-L1 expression, 3) tumor mutation burden (TMB) and 4) platinum sensitivity. We defined PD-L1 positivity as PD-L1 expression in ≥5% of immune cells or ≥1% of tumor cells, as this was the most common definition throughout the studies. Trials that defined PD-L1 positivity differently were not included because of insufficient studies with the same definition. We defined high TMB as 10 or more somatic mutations per Mb of DNA. This was consistent across the articles.

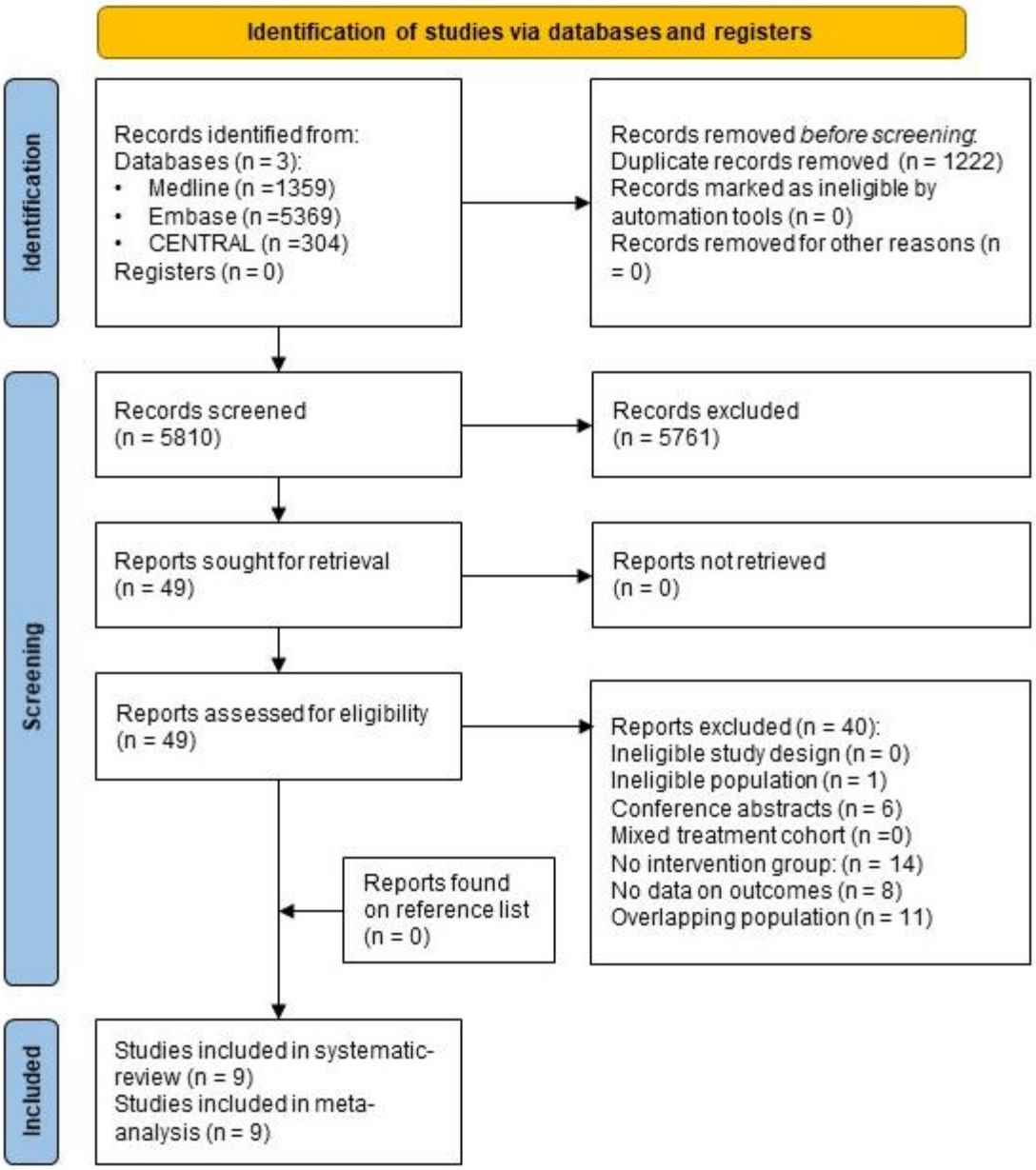

Figure 8. PRISMA flow chart

The rate of adverse events was calculated regardless of the best percentage change from baseline (BPCh) or the best overall response (BOR). We measured the rate of any grade of adverse events and the rate of serious adverse events. The rate of grade 3 or higher events was unavailable due to insufficient studies.

As we assumed considerable between-study heterogeneity at all cases, a random-effects model was used to pool effect sizes.

Proportions (objective response rate (ORR), disease control rate (DCR), presence of adverse events used for the main effect size measure with 95% confidence interval (CI). To calculate the study proportions, and the pooled proportions, the total number of patients and those with the event of interest was extracted from the studies.

We performed two main kinds of analyses for proportions. “Classical 2 level” meta-analyses were performed for pooling proportions separately. To gather more information and to be able

to make - although indirect - comparisons, a "3 level" model was used - where more results are available in the same study in separate categories (subgroups).
For time-to-event data an estimation for distribution-free pooled survival curves was performed using the method implemented by Pandey1 ("curve estimate"). Based on that we estimated the median survival time and its 95% CI (if it was suitable).
Results were considered statistically significant if the pooled CI did not contain the null value. We summarized the findings in tables, on forest plots, Kaplan-Meier plots (using Kaplan-Meier estimates), and estimated survival curves. If appropriate, between-study heterogeneity was described by the between-study variance (τ^2) and I^2statistics too, based on the classical model, and 3 level model. For IPD based results we reported only a point estimate for I^2 statistics. We reported the prediction interval if it is meaningful (there was enough study and with not too high heterogeneity).
Small study publication bias was assessed by visual inspection of funnel-plots and calculating modified Egger's test p-value. Although, we kept in mind that the test has limited diagnostic assessment below ~10 study, or ~ 25 study records. Potential outlier publications were explored using different influence measures and plots following the recommendation of Harrer et. al [15]. For time-to-event data the study number was too small to perform such an analysis.
All statistical analyses were made with R3 (v4.3.3) using the meta4 (v7.0.0) for 2 level models, metafor5 (v4.4.0) for 3 level models, dmetar6 (v0.1.0) and ggplot27 (v3.5.0) packages for influential analyses and plots. The survival curves were estimated using the package metaSurvival1 (v0.1.0)
We found 9 articles including the results of ovarian cancer. (Table 2.) The earliest published article was in 2017; the rest were since 2019, indicating that combination therapy is a newfound strategy. All 9 studies were clinical studies of phases 1 and 2. Only one study was a pure phase 1 study. One study was randomized, and the rest were not randomized. Some studies had multiple cohorts, with various dosages, multiple cancer types, or multiple arms. (Table 3.) As the studies were all in the early phase, the sample size was not significant individually, indicating this meta-analysis study may elucidate where the combination therapy stands.

Table 2. Selected articles

First author	**Year**	**Journal**	**Phase**	**Randomization**
Alison M. Schram [16]	2023	JAMA Oncology	2b	NO
Erika J. Lampert [17]	2020	Clin Cancer Res.	2	NO
Jung-Min Lee [18]	2017	Journal of Clinical Oncology	1	NO
Leslie M. Randall [19]	2023	Gynecologic Oncology	2	NO
Michael Friedlander [20]	2019	Lancet Oncol	1a/b	NO
Panagiotis A. Konstantinopoulos [21]	2019	JAMA Oncology	1,2	NO
Timothy A. Yap [22]	2022	JAMA Oncology	1b/2	NO
Yoo-Na Kim [23]	2023	International Journal of Cancer	2	YES
Yvette Drew [24]	2024	Clin Cancer Res.	2	NO

Table 3. Details of selected studies

First author	Treatment	Subgroups	#total patients	#relevant patients
Alison M. Schram	Talazoparib + Avelumab	BRCAm, PD-L1, TMB	200	26
Erika J. Lampert	Olaparib + Durvalumab	BRCAm, BRCAw/HRD+, HRD-, PD-L1, TMB	35	35
Jung-Min Lee	Olaparib + Durvalumab	BRCAm, BRCAw/HRD+, HRD-, PD-L1	26	12
Leslie M. Randall	Niraparib + Dostarlimab	n/a	41	41
Michael Friedlander	Pamiparib + Tislelizumab	BRCAm, BRCAw/HRD+, HRD-	49	49
Panagiotis A. Konstantinopoulos	Niraparib + Pembrolizumab	BRCAm, BRCAw/HRD+, HRD-, PD-L1	62	53
Timothy A. Yap	Talazoparib + Avelumab	BRCAm, BRCAw/HRD, HRD-, PD-L1, TMB	223	31
Yoo-Na Kim	Olaparib + Durvalumab	BRCAm, BRCAw/HRD+, PD-L1, TMB	30	12
Yvette Drew	Olaparib + Durvalumab	BRCAm, PD-L1	114	83

We summarized the effect of ORR and DCR according to the following: best percentage change from baseline (BPCh) or best overall response (BOR), genetic type, platinum sensitivity, or molecular expression patterns. The rate of adverse events was only summarized according to the best percentage change from baseline (BPCh) or best overall response (BOR). The meta-analysis of outcomes was further divided into BPCh and BOR subgroups. By principle, ORR can only be measured with the BORs; however, due to the inconsistency across studies regarding the reported outcomes, we decided to include data on BPCh, although there are limitations to the interpretation of the point estimates and the confidence intervals accordingly. In the present grant report, we present the results of the BOR dataset. Confidence interval estimation was influenced by the low number of studies and cases, and reported ORRs being 0 or1 in several cases, leading to wide confidence intervals.

Data for overall survival and progression free survival was collected. The analysis on overall survival was not conclusive due to the low number of available data (3 studies), and high heterogeneity. Progression free survival, independently of any previously specified subgroups, was 5.11 [2.55; 12.66] months based on 4 studies reporting this outcome, with moderate inter-study heterogeneity. (Figure 9.)

The ORR for BOR for the BRCAm subgroup was 0.48 [0.22;0.76], whereas for the BRCA wild type groups it was only 0.15 [0.05;0.37] and 0.16 [0.07;0.31] in the HDR+ and HDR- subgroups respectively. The heterogeneity of the studies is possibly deriving from the low number of reported patients, wide recruitment criteria and differences in PARPi and ICI choice. High heterogeneity in the BRCAm subgroup may originate from data in Drew Y. et al 2024 including only BRCAm, platinum sensitive patients compared to other studies with more divers patients. Although direct comparison is not possible in this dataset, results suggest that PARPi and ICI inhibitor co-therapy might be more effective in BRCAm ovarian cancer. (Figure 10.)

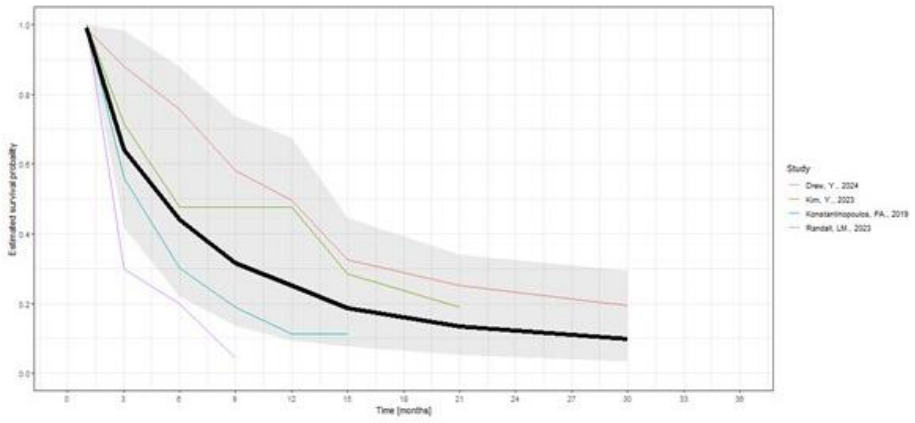

Median survival time (months) with 95% CI: 5.11 [2.55 - 12.66]
Point estimate for the I-squared statistics: 49.18 %

Figure 9. Progression free survival of ovarian cancer patients receiving the combination therapy of PARPi and ICI.

Panel A. ORR of BRCAm from BOR

Study	Event	Sample Size	ORR	Proportion	95%-CI
Lee, JM., 2017	0	2		0.00	[0.00; 0.84]
Konstantinopoulos, PA., 2019	2	11		0.18	[0.02; 0.52]
Schram, AM., 2022	5	18		0.28	[0.10; 0.53]
Lampert, EJ., 2020	3	8		0.38	[0.09; 0.76]
Friedlander, M., 2019	2	4		0.50	[0.07; 0.93]
Kim, Y., 2023	6	10		0.60	[0.26; 0.88]
Yap, TA., 2022	7	11		0.64	[0.31; 0.89]
Drew, Y., 2024	47	51		0.92	[0.81; 0.98]
Random effect				**0.48**	**[0.22; 0.76]**
I^2 = 77% [53%; 88%], τ = 1.21					

Panel B. ORR of BRCAw HDR+ from BOR

Study	Event	Sample Size	ORR	Proportion	95%-CI
Lampert, EJ., 2020	0	4		0.00	[0.00; 0.60]
Konstantinopoulos, PA., 2019	1	10		0.10	[0.00; 0.45]
Kim, Y., 2023	0	2		0.00	[0.00; 0.84]
Yap, TA., 2022	1	5		0.20	[0.01; 0.72]
Friedlander, M., 2019	2	9		0.22	[0.03; 0.60]
Lee, JM., 2017	1	4		0.25	[0.01; 0.81]
Random effect				**0.15**	**[0.05; 0.37]**
I^2 = 0% [0%; 75%], τ = 0					

Panel C. ORR HDR- from BOR

Study	Event	Sample Size	ORR	Proportion	95%-CI
Lampert, EJ., 2020	2	23		0.09	[0.01; 0.28]
Konstantinopoulos, PA., 2019	6	32		0.19	[0.07; 0.36]
Yap, TA., 2022	3	15		0.20	[0.04; 0.48]
Lee, JM., 2017	1	4		0.25	[0.01; 0.81]
Friedlander, M., 2019	0	1		0.00	[0.00; 0.97]
Random effect				**0.16**	**[0.07; 0.31]**
I^2 = 0% [0%; 79%], τ = 0					

Figure 10. ORR of BOR in BRCA mutant, in BRCA wild type but HDR positive, and in HDR negative ovarian cancer.

A more direct comparison was possible by using the 3-level statistical method, comparing inter-study subgroups along the included studies where multiple subgroups were available within studies. The 3-level analysis showed significant differences between these three subgroups (p=0.0162), supporting the hypothesis of higher efficacy of the combination therapy in BRCA mutant ovarian cancer. (Figure 11.)

The ORR of BOR for PD-L1+ and PD-L1- subgroups was similar; 0.51[0.02-.098] and 0.49[0.08-0.92] respectively. High heterogeneity is also present in this sub analysis. Again, direct comparison is not possible, however the results suggest that there is no substantial difference in the efficacy of the combination therapy in PD-L1+ and PD-L1- ovarian cancer. (Figure 12.)

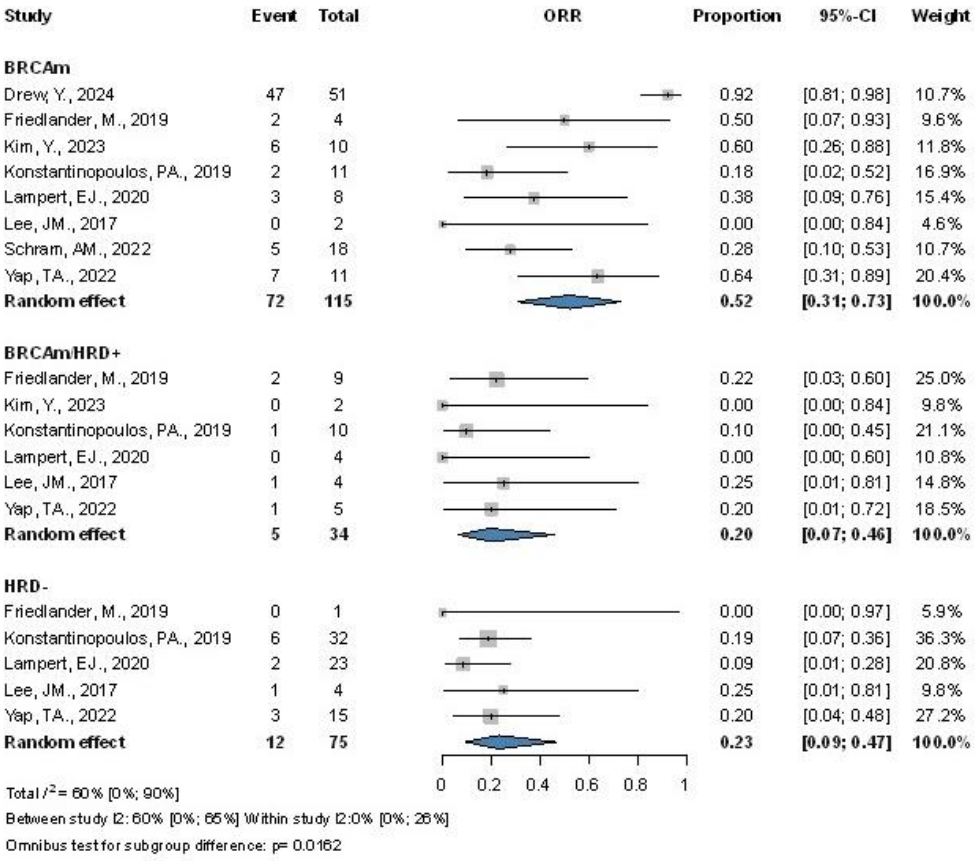

Figure 11. 3-level analysis of ORR of BOR in BRCAm, BRCAw HDR+ and HDR negative subgroups.

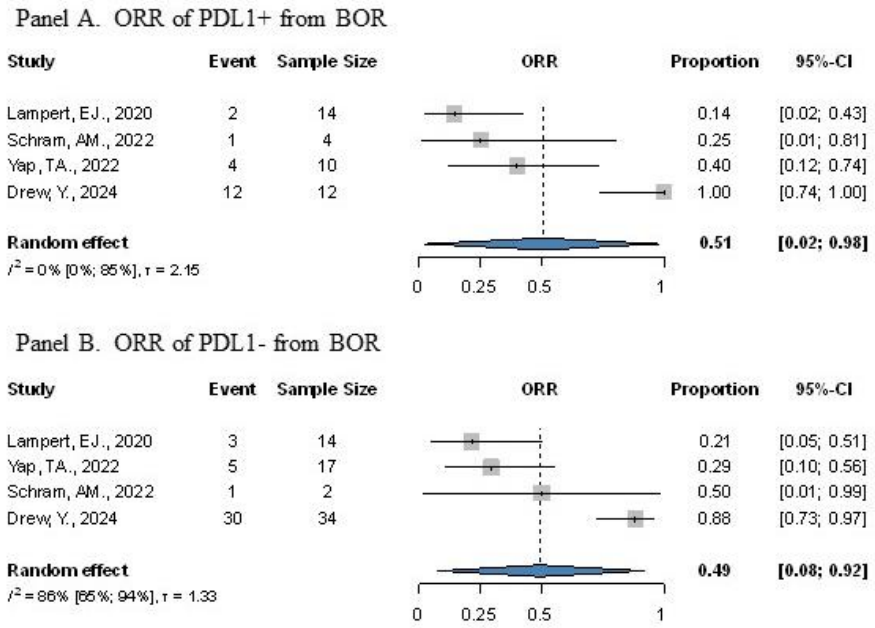

Figure 12. ORR of BOR in PD-L1+ and PD-L1- ovarian cancer.

Platinum sensitive and resistant subgroups were also analyzed. While platinum sensitive ovarian cancer patients had an ORR of BOR of 0.52 [0.16; 0.87], platinum resistant patients had only 0.2 [0.10; 0.36]. Direct statistical comparison was not possible here either, however; the data may suggest that the combination therapy might be more efficient in the generally more responsive platinum sensitive ovarian cancer. (Figure 13.)

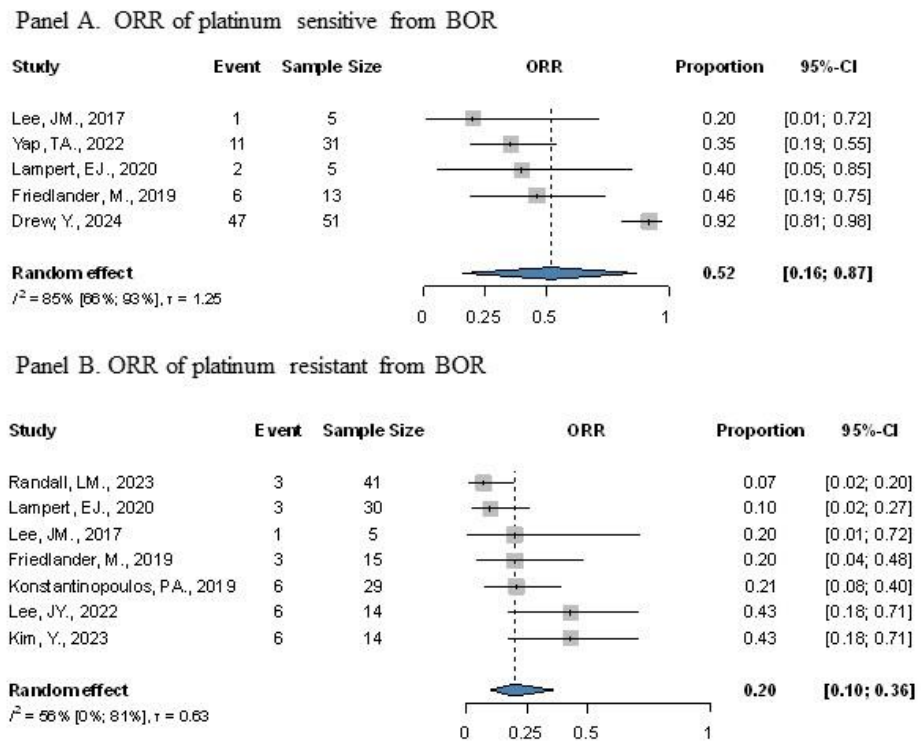

Figure 13. ORR of BOR in platinum sensitive and platinum resistant ovarian cancer.

PARPi have known for their various side effects involving the gastrointestinal tract and hematopoiesis. Most common adverse events are nausea, vomiting, constipation, diarrhea, anemia, leukopenia, neutropenia, and thrombocytopenia. They have beneficial effects on cancer

outcomes, but have higher risk of side effects, however; these side effects rarely lead to the complete discontinuation of the treatment [25]. The present meta-analysis also found high ORR of side effects of 1 [0.15;1], and about ORR of 0.35 [0.16;0.60] for serious side effects, including (Leslie M. Randall, 2023) that was stopped for futility. (Figure 14.)

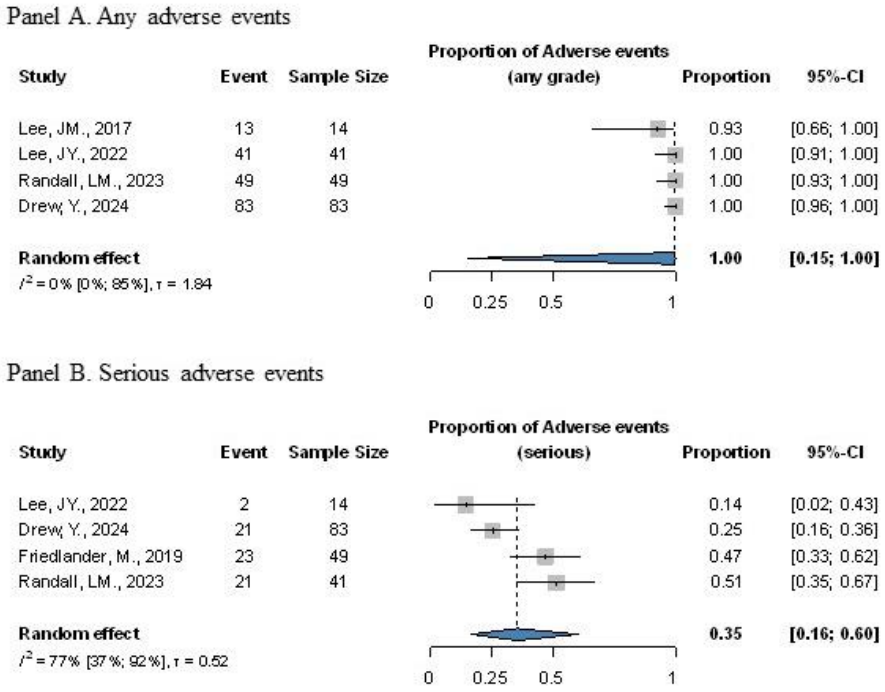

Figure 14. Adverse outcomes.

Risk of bias assessment of single arm studies was done using a modified version of modified Cowley's criteria composed of 14 questions, scoring 0: no reporting, 1: partial reporting or 2: satisfactory reporting [26]. Question 6 was divided into two separate questions: 6.1. Was the study powered for efficacy (2: powered for efficacy, 1: powered for efficacy but recruitment not completed (Drew Y. 2004) OR powered for safety OR not powered but interim analysis planned (Randall LM. 2023) 6.2. Was the statistical analysis valid and reported transparently? Question 10. asw modified to: Was the patient population identified? (Genotype, platinum sensitivity, etc.). In question 13. regarding the independence of investigators (conflict of interest) the following answer options were used: 2: no conflict of interest, 1: partial conflict of interest (funding received from the pharmaceutical company producing/patenting any of the used drugs. 0: absolute conflict of interest (have been employed by or owns stocks of pharmaceutical company producing/patenting any of the used drugs, in addition to receiving funding). Total score of 26-28 points means low risk of bias, 22-28 points mean moderate risk of bias, and <22 points mean high risk of bias. Based on this assessment, all articles had low or moderate risk of bias. (Figure 15.) The one included randomized control trial (Yoo-Na Kim, 2023) was analyzed by RoB2, and low risk of bias was concluded.

		Questions															
First author	Year	1	2	3	4	5	6.1	6.2	7	8	9	10	11	12	13	Total score	Risk of bias
Alison M. Schram	2022	2	2	2	2	2	2	2	2	2	2	2	2	2	0	26	low
Erika J. Lampert	2020	2	2	1	2	2	2	2	2	2	2	2	2	2	1	26	low
Jung-Min Lee	2017	2	2	1	2	2	0	2	2	2	2	2	2	2	0	23	moderate
Leslie M. Randall	2023	2	2	1	2	2	1	2	2	2	2	2	2	2	0	24	moderate
Michael Friedlander	2019	2	2	2	2	2	0	2	2	2	2	2	2	2	1	23	moderate
Panagiotis A. Konstantinopoulos	2019	2	2	2	2	2	2	2	2	2	2	2	2	2	1	27	low
Timothy A. Yap	2023	2	2	2	2	2	0	2	2	2	2	2	2	2	0	24	moderate
Yvette Drew	2024	2	2	1	2	2	1	2	2	2	2	2	2	2	0	24	moderate

Figure 15. Risk of bias analysis of single arm studies.

Our meta-analysis has several limitations: it is a single arm meta-analysis so no direct comparison is possible, the included studies involved low number of advanced ovarian cancer patients with divergent genetic background, platinum sensitivity, and previous treatments, also some of the studies were also not statistically powered for the reported outcomes. On the other hand, these data still imply that BRCAm and platinum sensitive ovarian cancer patients may have better response, while PD-L1 expression may not influence the efficacy of the combination therapy. Although our single arm meta-analysis has several limitations, the synthesis of these previous trials suggests that neither the ORR of BOR, nor the PFS of these patients are substantially higher compared to PARPi monotherapy for ovarian cancer maintenance therapy [25]. One of the included studies (Leslie M. Randall, 2023) was discontinued due to futility. Several randomized controlled trials are registered as ongoing trials comparing PARPi monotherapy and PARPi and ICI combination therapy, their results may clarify the possible synergistic effect of PARPi and ICI.

IV. The effect of poly(ADP-ribose) polymerase inhibition in rodent models of inflammatory bowel disease: a systematic review and meta-analysis (PROSPERO 2023 CRD42023461581)

Review question: Does the disruption of poly(ADP-ribose) polymerase enzyme activation have a generic protective effect in rodent models of inflammatory bowel disease (IBD) compared to healthy controls?
Animals/population: Inclusion criteria: Rodents (mouse, rat) in models of IBD regardless of induction technique (all sexes). Exclusion criteria: Animals with co-morbidities; ex vivo, in vitro and in silico models.
Searches: We searched the following electronic bibliographic databases on the 14th of February, 2024: MEDLINE, EMBASE, and Web of Science. The full search strategy is based on the search components “animal” (using PubMed and EMBASE search filters [ref, ref]), “poly(ADP-ribose) polymerase” and “inflammatory bowel disease”. (“inflammatory bowel” OR IBD OR Crohn OR colitis) AND ("poly(ADP-ribose)" or ADPRT or adp-ribose or PARP or Olaparib or Rucaparib or Niraparib or Talazoparib or PJ-34 or INO-1001 or 3-AB or 3-aminobenzamide). No publication date or language restrictions were applied. The number of total hits were 1036, out of which 346 was removed as duplicates. During title and abstract selection 662 additional records were excluded, so 26 records remained for full-text selection. During full-text selection additional 9 articles were excluded due to ineligible study design. We will screen the reference lists of included studies for additional eligible studies not retrieved by our search. The searches will be re-run just before the final analyses to retrieve the most recent studies eligible for inclusion. All procedures are done by two independent researchers (Máté

Bencsics and Rita Benkő), any inconsistencies in selection were addressed and resolved by a third party (Eszter M. Horváth)
Methods for data extraction: Two reviewers will independently extract data from each article. A third independent reviewer will resolve the disagreements. We first try to extract numerical data from tables, text or figures. If these are not reported, we will extract data from graphs using digital ruler software. In case data are not reported or unclear, we will attempt to contact authors by e-mail (max. 2 attempts). In case an outcome is measured at multiple time points, data from the time point where efficacy is highest will be included.
Data to be extracted: study design: Animal case-control studies, published in peer-reviewed papers will be reviewed. Experimental groups, control group(s) and number of animals per group as well as altogether will be extracted.
Planned approach: Both a qualitative and quantitative synthesis of the data will be performed if the included studies are sufficiently homogeneous. A meta-analysis will be performed for all outcome measures reported in at least three articles. If meta-analysis is not possible, data will be reported through a descriptive summary. The quantitative results will be summarized by calculating weighted mean differences or standardized mean differences using Stata 11 SE software (StataCorp LLC, College Station, TX, USA). Summary OR estimation, p value and 95% confidence interval (CI) will be calculated.

V. Other publications

During the grant period our working group in collaboration with the Translational Medicine Centre of Semmelweis University published two systematic review and meta-analyses in which this grant was cited. In both publications the PI of the present grant Eszter M. Horváth was the last or the corresponding author. This collaboration was a great opportunity to learn the methods and rigorous rules of conducting such studies. Following this joint project, we initiated two systematic review and meta-analyses within the scope of the present grant.
Greff D, Váncsa S, Váradi A, Szinte J, Park S, Hegyi P, Nyirády P, Ács N, Horváth EM, Várbíró S. **Myoinositols Prevent Gestational Diabetes Mellitus and Related Complications: A Systematic Review and Meta-Analysis of Randomized Controlled Trials.** Nutrients. 2023 Sep 30;15(19):4224. doi: 10.3390/nu15194224. **(IF: 5.9)**: According to the collected data, inositol, more precisely, myoinositol, as a supporting medication halves the risk of gestational diabetes mellitus in high-risk pregnancies and reduces the necessary insulin intake and other adverse outcomes (preeclampsia, gestational hypertension).
Greff D, Juhász AE, Váncsa S, Váradi A, Sipos Z, Szinte J, Park S, Hegyi P, Nyirády P, Ács N, Várbíró S, Horváth EM. **Inositol is an effective and safe treatment in polycystic ovary syndrome: a systematic review and meta-analysis of randomized controlled trials.** Reprod Biol Endocrinol. 2023 Jan 26;21(1):10. doi: 10.1186/s12958-023-01055-z. **(IF: 4.4)**: Inositol is an effective and safe treatment in polycystic ovary syndrome: a systematic review and meta-analysis of randomized controlled trials. According to the meta-analysis, inositol treatment has beneficial effects in the therapy of polycystic ovary syndrome (PCOS). As inositols were not inferior in comparison to metformin therapy, they should be included in the treatment protocol of PCOS, either as a co-treatment to metformin, or to prevent the side effects of metformin.

During the grant period our working group was also involved in studies in the related field of oxidative-nitrative stress and PARP activation in health and disease. Five additional publications were accepted citing the present grant, out of which in three, the PI of the present grant Eszter M. Horváth was the last or the corresponding author.

Bányai B, Répás C, Miklós Z, Johnsen J, Horváth EM, Benkő R. **Delta 9-tetrahydrocannabinol conserves cardiovascular functions in a rat model of endotoxemia: Involvement of endothelial molecular mechanisms and oxidative-nitrative stress.** PLoS One. 2023 Jun 16;18(6):e0287168. doi: 10.1371/journal.pone.0287168. **(IF: 3.7)**: A nonselective CB1/2R agonist–partial antagonist tetrahydrocannabinol(THC) showed potential therapeutic potential in a mild sepsis model. The THC pretreatment prevented a decline in cardiac filling and consequential decrement in stroke volume by maintaining endothelial function. This effect may have been due to lessened thromboxane A2 production and inducible cyclooxygenase expression, or the dampened oxidative-nitrative stress.

Bányai B, Vass Z, Kiss S, Balogh A, Brandhuber D, Karvaly G, Kovács K, Nádasy GL, Hunyady L, Dörnyei G, Horváth EM, Szekeres M. **Role of CB1 Cannabinoid Receptors in Vascular Responses and Vascular Remodeling of the Aorta in Female Mice**. Int J Mol Sci. 2023 Nov 17;24(22):16429. doi: 10.3390/ijms242216429. **(IF: 5.6)**: Genetic absence of cannabinoid receptor 1 led to a functional and structural difference between the KO. mice and their wild-type counterparts. Interestingly, lack of the CB1 led to an enhanced vasorelaxation mediated by both NO and prostaglandins; also, a smaller intima-media ratio was characteristic.

Vezér M, Jósvai A, Bányai B, Ács N, Keszthelyi M, Soltész-Katona E, Szekeres M, Oláh A, Radovits T, Merkely B, Horváth EM, Nádasy GL, Török M, Várbíró S. **Impact of Sex and Exercise on Femoral Artery Function: More Favorable Adaptation in Male Rats.** Life (Basel). 2023 Mar 13;13(3):778. doi: 10.3390/life13030778. **(IF: 3.2)** Sex hormones can have a beneficial effect on eNOS, COX, and COX-2 signaling. As a result of swim training, endothelial vasodilator substances were more abundant in male and female rats. In male rats, training led to a higher relaxation reserve capability along with NO-dependent relaxation, suggesting higher benefit of training.

Süli A, Magyar P, Vezér M, Bányai B, Szekeres M, Sipos M, Mátrai M, Hetthéssy JR, Dörnyei G, Ács N, Horváth EM, Nádasy GL, Várbíró S, Török M. **Effects of Gender and Vitamin D on Vascular Reactivity of the Carotid Artery on a Testosterone-Induced PCOS Model.** Int J Mol Sci. 2023 Nov 21;24(23):16577. doi: 10.3390/ijms242316577. **(IF: 5.6)** Vitamin D deficiency decreased estrogen- and testosterone-induced relaxation of isolated carotid arteries, although we detected a higher estrogen receptor density in these animals. On the other hand, testosterone treatment increased angiotensin-induced vasoconstriction and an enhanced androgen receptor density. We also detected a significant gender-related difference in the effects of Vitamin D hypovitaminosis.

Gerszi D, Orosz G, Török M, Szalay B, Karvaly G, Orosz L, Hetthéssy J, Vásárhelyi B, Török O, Horváth EM, Várbíró S. **Risk Estimation of Gestational Diabetes Mellitus in the First Trimester.** J Clin Endocrinol Metab. 2023 Oct 18;108(11):e1214-e1223. doi: 10.1210/clinem/dgad301. **(IF: 5.8)**: Soluble urokinase plasminogen activator receptor (SuPAR), cortisol, cortisone, dehydroepiandrosterone sulfate (DHEAS), testosterone, dihydrotestosterone (DHT), total antioxidant capacity (TAC), 11-deoxycorticosterone, and 21-deoxycortisol were identified as potential risk estimation markers during the first trimester of pregnancy. A logistic regression model was build based on these new markers along with traditional predictors for clinically relevant early prediction of later-onset gestational diabetes mellitus. This study is based on the GIPS study from Hungary.

Limitations

Due to various, in the yearly reports already described obstacles, we were not able to perform all the planned experiments. First, our team encountered the delayed arrival of the transgenic mice, and the low reproduction rate of the animals. The pandemic also substantially hindered our project. During the lock-down, we had to suspend our experiments. When university employees could continue the research, we could still work at a slower pace due to the absence of PhD and graduate students. Later, the overload of supply systems that distribute health and research reagents, and the following inflation and price increase also hindered our work. Tragically, we lost one of the leading investigators, as Prof. Dr. Gábor Veres passed away. After the thorough evaluation of our progress, we decided to apply for grant period extension, however; we had to face the consequences of the experiment suspension and technical difficulties. We decided to introduce a new method to the working group; systematic review and meta-analysis, resulting in 2 already publishes articles not strictly related to the present grant, but making us competent to execute two systematic review and meta-analyses within the scope of the present grant. Our working group also continued its research in the related field of oxidative-nitrative stress and PARP activation in health and disease, leading to 5 additional publications.

References

1 Zingarelli, B. *et al.* Activator protein-1 signalling pathway and apoptosis are modulated by poly(ADP-ribose) polymerase-1 in experimental colitis. *Immunology* **113**, 509-517, doi:10.1111/j.1365-2567.2004.01991.x (2004).

2 Zingarelli, B., O'Connor, M. & Hake, P. W. Inhibitors of poly (ADP-ribose) polymerase modulate signal transduction pathways in colitis. *Eur J Pharmacol* **469**, 183-194, doi:10.1016/s0014-2999(03)01726-6 (2003).

3 Markowitz, M. M., Rozen, P., Pero, R. W., Tobi, M. & Miller, D. G. Hydrogen peroxide induced adenosine diphosphate ribosyl transferase (ADPRT) response in patients with inflammatory bowel disease. *Gut* **29**, 1680-1686, doi:10.1136/gut.29.12.1680 (1988).

4 Decker, P. *et al.* Zinc is an essential cofactor for recognition of the DNA binding domain of poly(ADP-ribose) polymerase by antibodies in autoimmune rheumatic and bowel diseases. *Arthritis Rheum* **41**, 918-926, doi:10.1002/1529-0131(199805)41:5<918::Aid-art20>3.0.Co;2-w (1998).

5 Reumaux, D., Mézière, C., Colombel, J. F., Duthilleul, P. & Mueller, S. Distinct production of autoantibodies to nuclear components in ulcerative colitis and in Crohn's disease. *Clin Immunol Immunopathol* **77**, 349-357, doi:10.1006/clin.1995.1162 (1995).

6 Judit Béres, N. *et al.* Role of microRNA-223 in the regulation of poly(ADP-ribose) polymerase in pediatric patients with Crohn's disease. *Scand J Gastroenterol* **53**, 1066-1073, doi:10.1080/00365521.2018.1498915 (2018).

7 Bettelli, E. *et al.* Reciprocal developmental pathways for the generation of pathogenic effector TH17 and regulatory T cells. *Nature* **441**, 235-238, doi:10.1038/nature04753 (2006).

8 Rovedatti, L. *et al.* Differential regulation of interleukin 17 and interferon gamma production in inflammatory bowel disease. *Gut* **58**, 1629-1636, doi:10.1136/gut.2009.182170 (2009).

9 Ahmad, S. F., Zoheir, K. M., Bakheet, S. A., Ashour, A. E. & Attia, S. M. Poly(ADP-ribose) polymerase-1 inhibitor modulates T regulatory and IL-17 cells in the prevention of adjuvant induced arthritis in mice model. *Cytokine* **68**, 76-85, doi:10.1016/j.cyto.2014.04.006 (2014).

10 Kamboj, A. *et al.* Poly(ADP-ribose) polymerase 2 contributes to neuroinflammation and neurological dysfunction in mouse experimental autoimmune encephalomyelitis. *J Neuroinflammation* **10**, 49, doi:10.1186/1742-2094-10-49 (2013).

11 Blagov, A. *et al.* Novel Models of Crohn's Disease Pathogenesis Associated with the Occurrence of Mitochondrial Dysfunction in Intestinal Cells. *Int J Mol Sci* **23**, doi:10.3390/ijms23095141 (2022).

12 Veneziani, A. C., Scott, C., Wakefield, M. J., Tinker, A. V. & Lheureux, S. Fighting resistance: post-PARP inhibitor treatment strategies in ovarian cancer. *Therapeutic advances in medical oncology* **15**, 17588359231157644, doi:10.1177/17588359231157644 (2023).
13 Naini, B. V. & Cortina, G. A histopathologic scoring system as a tool for standardized reporting of chronic (ileo)colitis and independent risk assessment for inflammatory bowel disease. *Hum Pathol* **43**, 2187-2196, doi:10.1016/j.humpath.2012.03.008 (2012).
14 Peyraud, F. & Italiano, A. Combined PARP Inhibition and Immune Checkpoint Therapy in Solid Tumors. *Cancers* **12**, doi:10.3390/cancers12061502 (2020).
15 Harrer, M., Cuijpers, P., Furukawa, T., & Ebert, D. *Doing Meta-Analysis with R: A Hands-On Guide (1st ed.)*. (Chapman and Hall/CRC., 2021).
16 Schram, A. M. *et al.* Avelumab Plus Talazoparib in Patients With BRCA1/2- or ATM-Altered Advanced Solid Tumors: Results From JAVELIN BRCA/ATM, an Open-Label, Multicenter, Phase 2b, Tumor-Agnostic Trial. *JAMA Oncol* **9**, 29-39, doi:10.1001/jamaoncol.2022.5218 (2023).
17 Lampert, E. J. *et al.* Combination of PARP Inhibitor Olaparib, and PD-L1 Inhibitor Durvalumab, in Recurrent Ovarian Cancer: a Proof-of-Concept Phase II Study. *Clin Cancer Res* **26**, 4268-4279, doi:10.1158/1078-0432.Ccr-20-0056 (2020).
18 Lee, J. M. *et al.* Safety and Clinical Activity of the Programmed Death-Ligand 1 Inhibitor Durvalumab in Combination With Poly (ADP-Ribose) Polymerase Inhibitor Olaparib or Vascular Endothelial Growth Factor Receptor 1-3 Inhibitor Cediranib in Women's Cancers: A Dose-Escalation, Phase I Study. *J Clin Oncol* **35**, 2193-2202, doi:10.1200/jco.2016.72.1340 (2017).
19 Randall, L. M. *et al.* Niraparib and dostarlimab for the treatment of recurrent platinum-resistant ovarian cancer: results of a Phase II study (MOONSTONE/GOG-3032). *Gynecol Oncol* **178**, 161-169, doi:10.1016/j.ygyno.2023.10.005 (2023).
20 Friedlander, M. *et al.* Pamiparib in combination with tislelizumab in patients with advanced solid tumours: results from the dose-escalation stage of a multicentre, open-label, phase 1a/b trial. *Lancet Oncol* **20**, 1306-1315, doi:10.1016/s1470-2045(19)30396-1 (2019).
21 Konstantinopoulos, P. A. *et al.* Single-Arm Phases 1 and 2 Trial of Niraparib in Combination With Pembrolizumab in Patients With Recurrent Platinum-Resistant Ovarian Carcinoma. *JAMA Oncol* **5**, 1141-1149, doi:10.1001/jamaoncol.2019.1048 (2019).
22 Yap, T. A. *et al.* Avelumab Plus Talazoparib in Patients With Advanced Solid Tumors: The JAVELIN PARP Medley Nonrandomized Controlled Trial. *JAMA Oncol* **9**, 40-50, doi:10.1001/jamaoncol.2022.5228 (2023).
23 Kim, Y. N. *et al.* Randomized, two-arm, noncomparative phase 2 study of olaparib plus cediranib or durvalumab in HRR-mutated, platinum-resistant ovarian cancer: A substudy of KGOG 3045. *Int J Cancer* **153**, 2032-2044, doi:10.1002/ijc.34696 (2023).
24 Drew, Y. *et al.* Olaparib plus Durvalumab, with or without Bevacizumab, as Treatment in PARP Inhibitor-Naïve Platinum-Sensitive Relapsed Ovarian Cancer: A Phase II Multi-Cohort Study. *Clin Cancer Res* **30**, 50-62, doi:10.1158/1078-0432.Ccr-23-2249 (2024).
25 Hao, J. *et al.* Efficacy and safety of PARP inhibitors in the treatment of advanced ovarian cancer: An updated systematic review and meta-analysis of randomized controlled trials. *Critical reviews in oncology/hematology* **157**, 103145, doi:10.1016/j.critrevonc.2020.103145 (2021).
26 Alsinbili, A. Assessing the risk of bias in single-arm trials for systematic reviews: moving towards a more reliable evaluation of clinical evidence. *Future healthcare journal* **10**, 26-27, doi:10.7861/fhj.10-3-s26 (2023).